NUMERICAL SIMULATION OF THE TAYLOR-GREEN VORTEX

Steven A. Orszag
Department of Mathematics
Massachusetts Institute of Technology
Cambridge, Massachusetts, 02139 U.S.A.

INTRODUCTION

In a classic paper, Taylor and Green (1937) considered the dynamical evolution of a model three-dimensional vortex field in order to clarify the dynamics of turbulence. The Taylor-Green vortex illustrates in a relatively simple flow the basic turbulence decay mechanisms of the production of small eddies and the enhancement of dissipation by the stretching of vortex lines. It has also proved exceedingly useful for testing numerical and perturbation methods, as discussed later in this paper.

In the Taylor-Green vortex, the initial physical-space velocity field is

$$v_1(x_1,x_2,x_3) = \cos x_1 \sin x_2 \cos x_3 \qquad (1a)$$

$$v_2(x_1,x_2,x_3) = -\sin x_1 \cos x_2 \cos x_3 \qquad (1b)$$

$$v_3(x_1,x_2,x_3) = 0 \; , \qquad (1c)$$

where we have shifted the origin of x_3 by $\frac{1}{2}\pi$ from the initial conditions chosen by Taylor and Green for convenience in developing a numerical method (see below). The initial vorticity field $\vec{\omega} = \vec{\nabla} \times \vec{v}$ is

$$\omega_1(x_1,x_2,x_3) = -\sin x_1 \cos x_2 \sin x_3 \qquad (2a)$$

$$\omega_2(x_1,x_2,x_3) = -\cos x_1 \sin x_2 \sin x_3 \qquad (2b)$$

$$\omega_3(x_1,x_2,x_3) = -2\cos x_1 \cos x_2 \cos x_3 \qquad (2c)$$

Although the streamlines of the initial velocity field (1) are the planar curves $\cos x_1 \cos x_2 = $ const in the planes $x_3 = $ const, the flow that develops from (1) is three-dimensional. The initial vortex

lines are the curves $\sin x_1 / \sin x_2 = \text{const}$, $\sin^2 x_1 \cos x_3 = \text{const}$ so they are twisted and may induce a velocity field to stretch themselves. In fact, since $\vec{\omega} \cdot \vec{\nabla} \vec{v}$ is initially nonzero such stretching does take place. Also, since the initial value of $(\vec{v} \times \vec{\omega})_3$ is nonzero, a nonzero component v_3 develops after the initial instant and the field becomes truly three dimensional. The Taylor-Green vortex is perhaps the simplest example of self-induced vortex stretching by a three-dimensional velocity field.

The dynamical problem is to solve the Navier-Stokes equations for incompressible flow

$$\frac{\partial \vec{v}(\vec{x},t)}{\partial t} + \vec{v}(\vec{x},t) \cdot \vec{\nabla} \vec{v}(\vec{x},t) = - \vec{\nabla} p(\vec{x},t) + \frac{1}{R} \nabla^2 \vec{v}(\vec{x},t) \qquad (3)$$

$$\vec{\nabla} \cdot \vec{v}(\vec{x},t) = 0 , \qquad (4)$$

where $p(\vec{x},t)$ is the pressure (normalized by the density) and R is the Reynolds number, subject to the (incompressible) initial conditions (1). The boundary conditions on $\vec{v}(\vec{x},t)$ are implicitly taken to be periodic, $\vec{v}(\vec{x}+2\pi\vec{n},t) = \vec{v}(\vec{x},t)$ where $\vec{n}$ has integral components, because these are maintained in time evolution by (3), (4). The pressure field in (3) is effectively a 'Lagrange multiplier' that ensures compliance with the incompressibility constraint (4); the pressure may be eliminated from (3) by taking its divergence and applying (4).

Taylor and Green (1937) investigated the evolution of their vortex by developing a perturbation solution to (3), (4) in powers of the time t. They found that the mean-square vorticity $\Omega(t) = \overline{\omega^2}$, where the overbar indicates an average over a periodicity cube, is given by

$$\Omega(t) = \frac{3}{4} [1 - \frac{6t}{R} + (\frac{5}{48} + \frac{18}{R^2})t^2 - (\frac{5}{3} + \frac{36}{R^2}) \frac{t^3}{R}$$

$$+ (\frac{50}{99.64} + \frac{1835}{9.16R^2} + \frac{54}{R^4})t^4 + \ldots] \qquad (5)$$

The dynamical significance of $\Omega(t)$ is that, with periodic boundary conditions, $\Omega(t)$ is related to the rate of kinetic energy decay $\epsilon(t)$ by $\epsilon(t) = -\frac{d}{dt} \frac{1}{2} \overline{v^2} = \frac{1}{R} \Omega(t)$. It is clear that finite-order truncations of the series (5) cannot remain valid as $t \rightarrow \infty$ (since $\Omega \rightarrow 0$ as $t \rightarrow \infty$). Examination of (5) suggests that, as $R \rightarrow \infty$, the perturbation series in powers of t diverges for $t \gtrsim 3$.

Goldstein (1940) investigated the evolution of the Taylor-Green vortex by developing a perturbation series in powers of the Reynolds number R. He found

$$\Omega(t) = \frac{3}{4} [e^{-6t/R} - \frac{R^2}{384} (e^{-6t/R} - 20e^{-12t/R} + 35e^{-14t/R} - 16e^{-16t/R})$$

$$+ R^4 (\frac{4105}{635830272} e^{-6t/R} + \ldots) + \ldots] \qquad (6)$$

Notice that (6) is a more inclusive series than (5) in the sense that each term of (6) is a resummation of an infinite number of partial terms of (5); on the other hand, each term of (5) derives from only a finite number of terms of (6). Also, notice that finite order truncations of (6) do not have the secular behavior exhibited by truncations of (5) as $t \rightarrow \infty$. However, examination of the displayed terms of (6) suggests that for $t/R \gtrsim 1$, perturbation series in powers of R diverges for $R \gtrsim 20$.

Neither perturbation series in powers of t nor R can describe the evolution of the flow field for large t or R. In this paper, we study the Taylor-Green vortex by numerical solution of the Navier-Stokes equations. In addition to the fundamental fluid dynamical interest in the development of the Taylor-Green vortex, the flow is a most convenient one on which to debug and perform tests of sophisticated three-dimensional numerical hydrodynamics simulation codes. The present results were obtained by a very efficient and accurate method that is highly specialized to the Taylor-Green vortex and so not generalizable to a wide variety of flows. Nevertheless,

the present results have proved most useful in validation tests of a variety of more general simulation codes(Orszag and Patterson 1972).

NUMERICAL METHOD

The Navier-Stokes equations (3), (4) are solved by finite differences in t (using a second-order Adams-Bashforth scheme on the advective terms and Crank-Nicolson implicit differencing on the viscous terms) and a spectral (Fourier expansion) method in space. Because of spatial periodicity, the velocity field is expansible as

$$\vec{v}(\vec{x},t) = \sum \vec{u}(\vec{k},t)e^{i\vec{k}\cdot\vec{x}} \tag{7}$$

where $\vec{k}$ has integral components. The flow that develops from the initial conditions (1) has several symmetries and invariances that may be used to reduce the number of independent components in (7). These symmetries and invariances are

$$\vec{v}(\vec{x}) = -\vec{v}(-\vec{x}) \tag{8a}$$

$$v_i(x_1,x_2,x_3) = r_i v_i(x_1,x_2,-x_3) \tag{8b}$$

$$v_2(x_1,x_2,x_3) = v_1(x_2,-x_1,x_3), \quad v_3(x_1,x_2,x_3) = v_3(x_2,-x_1,x_3) \tag{8c}$$

$$v_i(x_1,x_2,x_3) = t_i v_i(x_1 + \pi, \pi - x_2, x_3 + \pi) \tag{8d}$$

where repeated latin indices are not summed, $r_1 = r_2 = t_1 = t_3 = 1$, $r_3 = t_2 = -1$, and

$$\vec{u}(\vec{k}) = 0 \tag{8e}$$

unless $k_1 \equiv k_2 \equiv k_3$ (mod 2). These relations are not all independent. For example, (8c), which states invariance of the flow under 90° rotations about the x_3-axis, applied twice gives $v_3(-x_1,-x_2,x_3) = v_3(x_1,x_2,x_3)$ which also follows from (8a) and (8b). The properties (8) imply that the velocity field of the Taylor-Green vortex is representable as

$$\left\{\begin{array}{l} v_1(x_1,x_2,x_3) \\ v_2(x_1,x_2,x_3) \\ v_3(x_1,x_2,x_3) \end{array}\right\}$$

$$= \sum_{m=0}^{\infty} \sum_{n=0}^{\infty} \sum_{p=0}^{\infty} \left\{\begin{array}{l} a_{mnp}^{(1)} \cos[(2m+1)x_1]\sin[(2n+1)x_2]\cos[(2p+1)x_3] \\ a_{mnp}^{(2)} \sin[(2m+1)x_1]\cos[(2n+1)x_2]\cos[(2p+1)x_3] \\ a_{mnp}^{(3)} \sin[(2m+1)x_1]\sin[(2n+1)x_2]\sin[(2p+1)x_3] \end{array}\right.$$

$$+ \left.\begin{array}{l} b_{mnp}^{(1)} \sin[2mx_1]\cos[2nx_2]\cos[2px_3] \\ b_{mnp}^{(2)} \cos[2mx_1]\sin[2nx_2]\cos[2px_3] \\ b_{mnp}^{(3)} \cos[2mx_1]\cos[2nx_2]\sin[2px_3] \end{array}\right\} \tag{9}$$

In order to obtain a finite approximation to $\vec{v}$, we truncate
the series (7) to the region $-K < k_\alpha < K$, $\alpha = 1,2,3$ denoted by
$||\vec{k}|| < K$, and apply the Galerkin procedure to get the equations
(Orszag 1971)

$$[\frac{\partial}{\partial t} + \frac{k^2}{R}]u_\alpha(\vec{k},t) = -ik_\beta(\delta_{\alpha\gamma} - \frac{k_\alpha k_\gamma}{k^2}) \sum_{\substack{\vec{p}+\vec{q}=\vec{k} \\ ||\vec{p}||,||\vec{q}||<K}} u_\beta(\vec{p},t)u_\gamma(\vec{q},t) \tag{10}$$

where repeated Greek indices are summed and the pressure has been
eliminated by means of the incompressibility constraint.

An efficient algorithm for computing the right-hand side of
(10) has been devised (Orszag 1971). It involves 12 real or
conjugate symmetric discrete Fourier transforms on $K \times K \times K$ points;
the Fourier transforms are performed by the fast Fourier transform
algorithm in order $K^3 \log_2 K$ arithmetic operations. This transform
method for the Taylor-Green vortex makes essential use of all the
symmetries (8); without (8), the most efficient transform method
for evaluation of the right-hand side of (10), which is the

pseudospectral method (Orszag 1971), would require 9 real or conjugate-symmetric discrete Fourier transforms on $2K \times 2K \times 2K$ points or roughly a factor 6 more work than involved in the Taylor-Green vortex. Another advantage of the spectral method just described for the Taylor-Green vortex is that it allows great reductions in the amount of computer storage necessary with a given spectral cutoff or spatial resolution $\Delta x = \pi/K$. In fact, the property (8e) alone gives a factor four reduction in the necessary storage space. Details on all the transform methods mentioned above are given elsewhere (Orszag 1971).

The spectral method discussed here has several important advantages over more conventional finite difference techniques (Orszag and Israeli 1974). For the Taylor-Green vortex, the spectral results are infinite-order accurate, i.e. errors go to zero faster than any finite power of $1/K$ as $K \to \infty$, in contrast to the finite order accuracy of difference schemes. The rapid convergence of the spectral results translates into more accurate simulations at finite resolution. In the 5-10% error range, spectral simulations require roughly a factor two less resolution in each space direction than finite-difference approximations or a factor eight fewer degrees of freedom [even without the symmetries (8)] in three dimensions. At higher accuracy, the advantages of spectral schemes are more pronounced. With $K = 16$ or $32,768$ Fourier modes to represent each component of the velocity field, the present spectral method requires $0.6s$ per time step on a CDC 7600 computer.

RESULTS

In Fig. 1, we plot the evolution of $\Omega(t)$ at $R = 200$ determined by perturbation series in t truncated at t^5 (curve 1), perturbation series in R truncated at R^4 (curve 2), and numerical

simulation with spectral cutoff K = 16 (curve 3). In the absence

of the nonlinear terms of the Navier-Stokes equations $\Omega(t) \leq \Omega(0)$,

so that the enhancement of mean square vorticity observed in Fig. 1

is a measure of the strength of the nonlinearity. In Fig. 2, a

similar plot is made for R = 300. Additional tests and comparisons

between runs of varying spatial resolution indicate that the numerical

simulation results should be accurate to within 2% at R = 200 and

5% at R = 300. An indication of the magnitude of the Reynolds

number R is given by the relation $R_\lambda = .372\ R$ at t = 0, where

R_λ is the Reynolds number based on the Taylor microscale (Batchelor

1953). Thus, at R = 200, $R_\lambda = 74$ at t = 0 and $R_\lambda = 26$ at

t = 6, while at R = 300, $R_\lambda = 112$ at t = 0 and $R_\lambda = 37$ at

t = 6. These values of R_λ should be compared with laboratory wind-

tunnel experiments on grid-generated turbulence which are generally

performed in the range $R_\lambda = 25\text{-}50$.

It is apparent from Figs. 1 and 2 that perturbation expansion

in powers of t is at least as good as that in powers of R at

these Reynolds numbers, despite the more inclusive nature of the R

expansion. Nevertheless, both expansions are woefully inadequate

to describe either the large t behavior or even the variation of

the maximum of $\Omega(t)$ with Reynolds number.

The variation of $\Omega(t)$ with Reynolds number relates indirectly

to the effect of Reynolds number on large scale structures in the

flow since $\varepsilon(t) = \frac{1}{R}\,\Omega(t)$. If $\Omega(t)$ is asymptotically proportional

to R (for t beyond some initial relaxation period) then $\varepsilon(t)$ is

Reynolds number independent. Some support for this behavior is

given by the results shown in Fig. 3. Here $\varepsilon(t)$ is plotted as a

function of t for R = 100-400, the simulation with R = 400

being only moderately accurate.

It appears that, as R → ∞, $\varepsilon(t)$ approaches a finite limiting

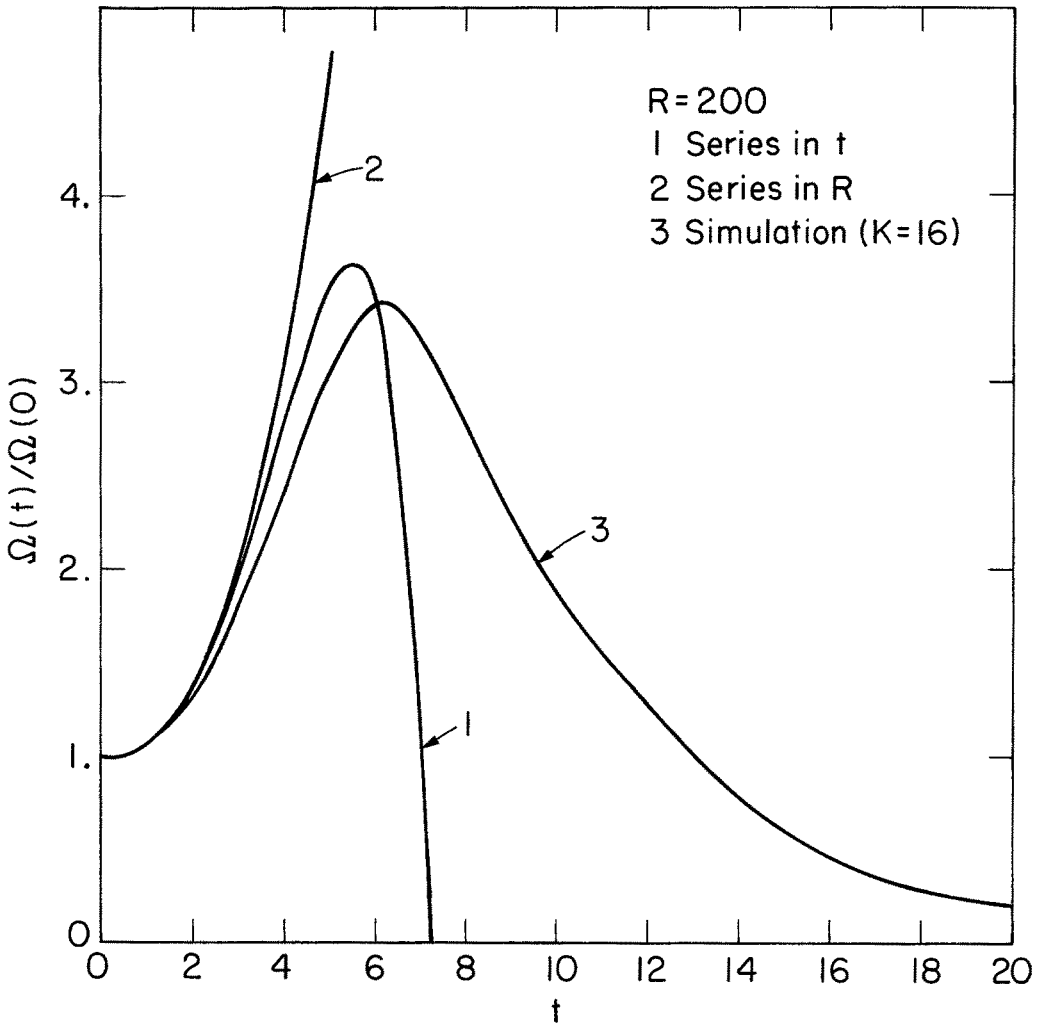function $\varepsilon_*(t)$ [probably with the property that $\varepsilon_*(t) = 0$ for

Fig. 1   Enhancement of mean-square vorticity $\Omega(t)/\Omega(0)$
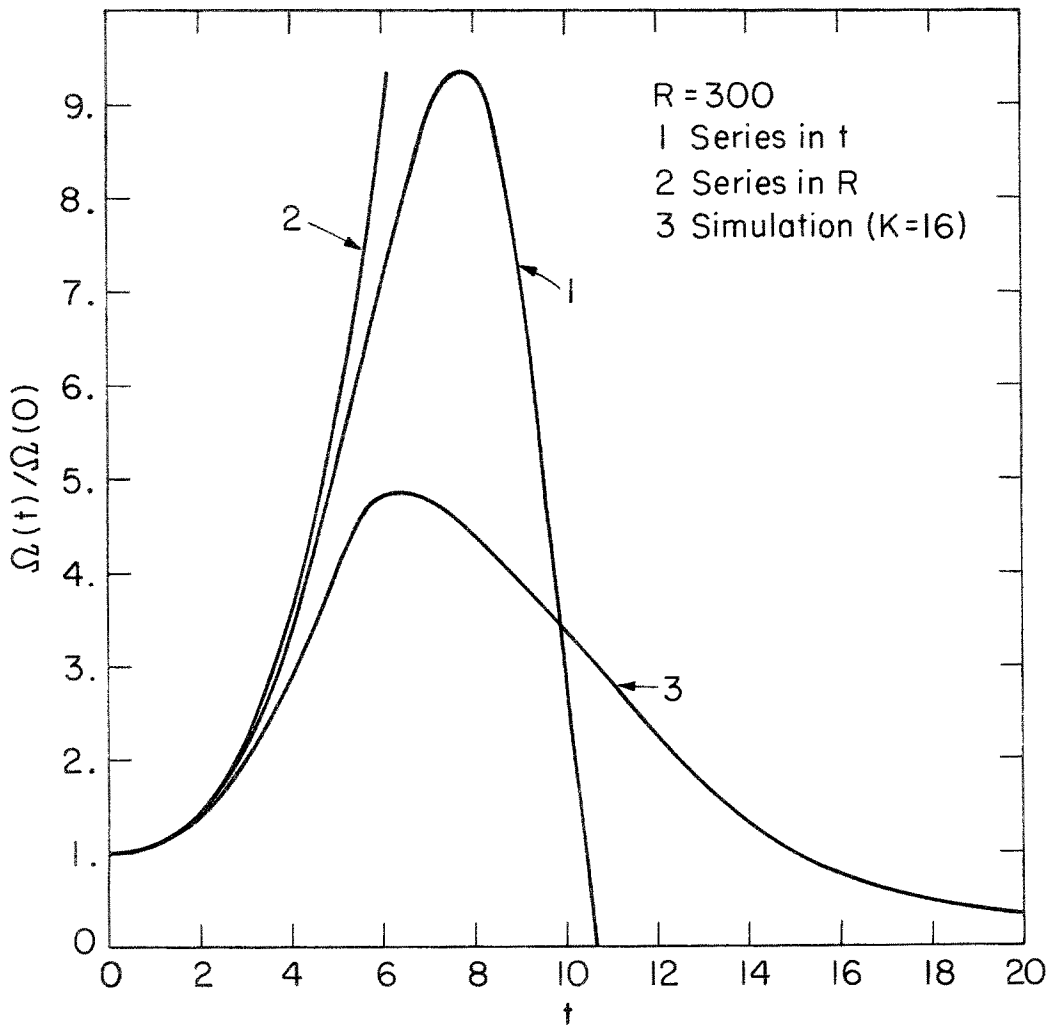versus   t   at   R = 200.

Fig. 2 Enhancement of mean-square vorticity $\Omega(t)/\Omega(0)$ versus t at R = 300.
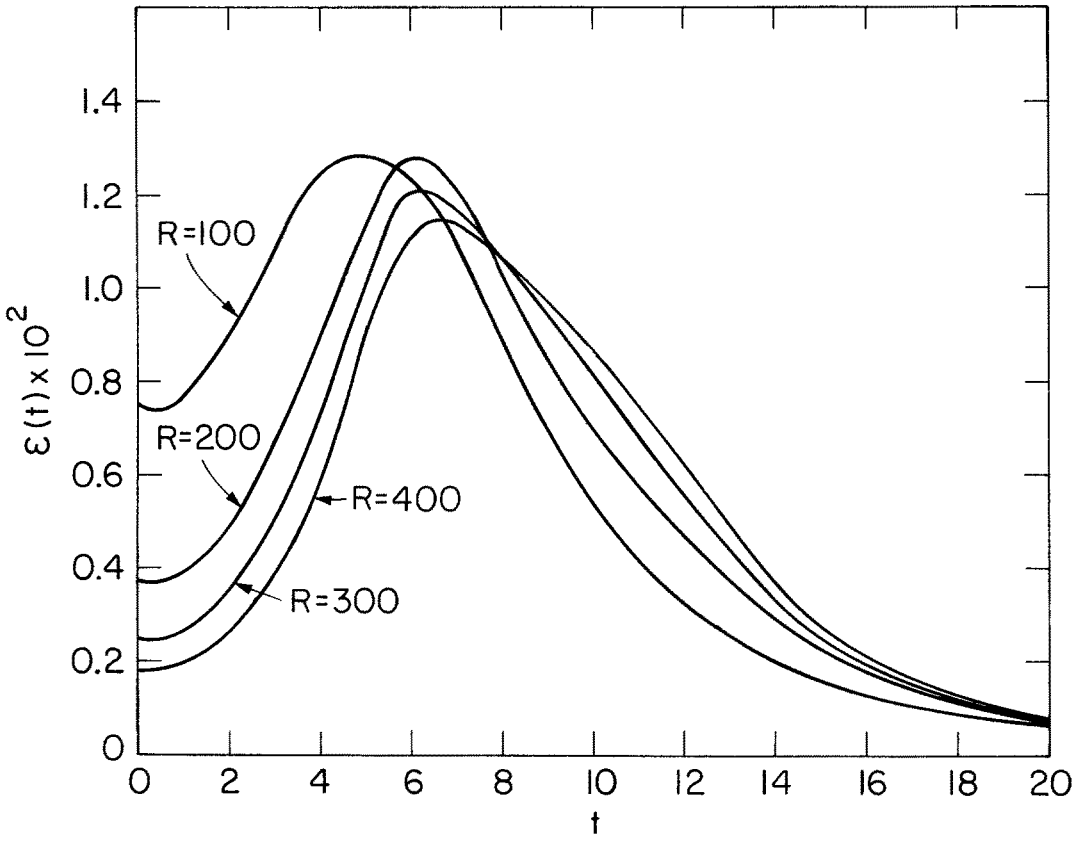
Fig. 3 Rate of energy dissipation $\epsilon(t)$ versus t for
R = 100, 200, 300, 400.

$t < t_*$, [where t_* is the time at which $\Omega(t)$ becomes infinite at $R = \infty$]. This result is extremely important as it demonstrates a large scale feature of the flow that is asymptotically Reynolds number independent. If all large scale features of turbulent flows are Reynolds number independent then it is possible to simulate large scale flow features of very high Reynolds number turbulence when the Reynolds number of the simulation (and, hence, the required resolution) is quite modest (cf. Orszag and Israeli 1974).

In Figs. 4 and 5, we show contour plots of v_1 and v_3, respectively, at $t = 3.5$, $R = 100$. These plots illustrate the character of the flow that develops from the initial conditions (1).

In Fig. 6, we show the evolution at $R = 200$ of

$$D3/D1 = \sum k^2 |u_3(\vec{k})|^2 / \sum k^2 |u_1(\vec{k})|^2 \tag{11a}$$

$$E3/E1 = \sum |u_3(k)|^2 / \sum |u_1(k)|^2 , \tag{11b}$$

which are, respectively, measures of the anisotropy of energy dissipation and energy. It is apparent that energy dissipation approaches a state of near isotropy for $t = 4-16$, while the kinetic energy itself is always far from isotropy. This result is consistent with ideas of turbulence theory on local equilibrium of small-scale eddies. As first proposed by Kolmogorov (Batchelor 1953), small eddies [which dominate dissipation because of the factors k^2 in (11a)] should approach isotropy and equilibrium in a time much shorter than the overall decay time of the turbulence. On the other hand, large eddies [which dominate the kinetic energy] evolve in the same time scale as the overall decay proceeds and no strong tendency to isotropy should be observed.

Finally, we remark that, as $t \to \infty$, the flow decays to a form proportional to the initial conditions (1) which is very anisotropic. At late times, R_λ is very small and viscous dissipation dominates the nonlinear terms in (3) so that the modes in (9) with the
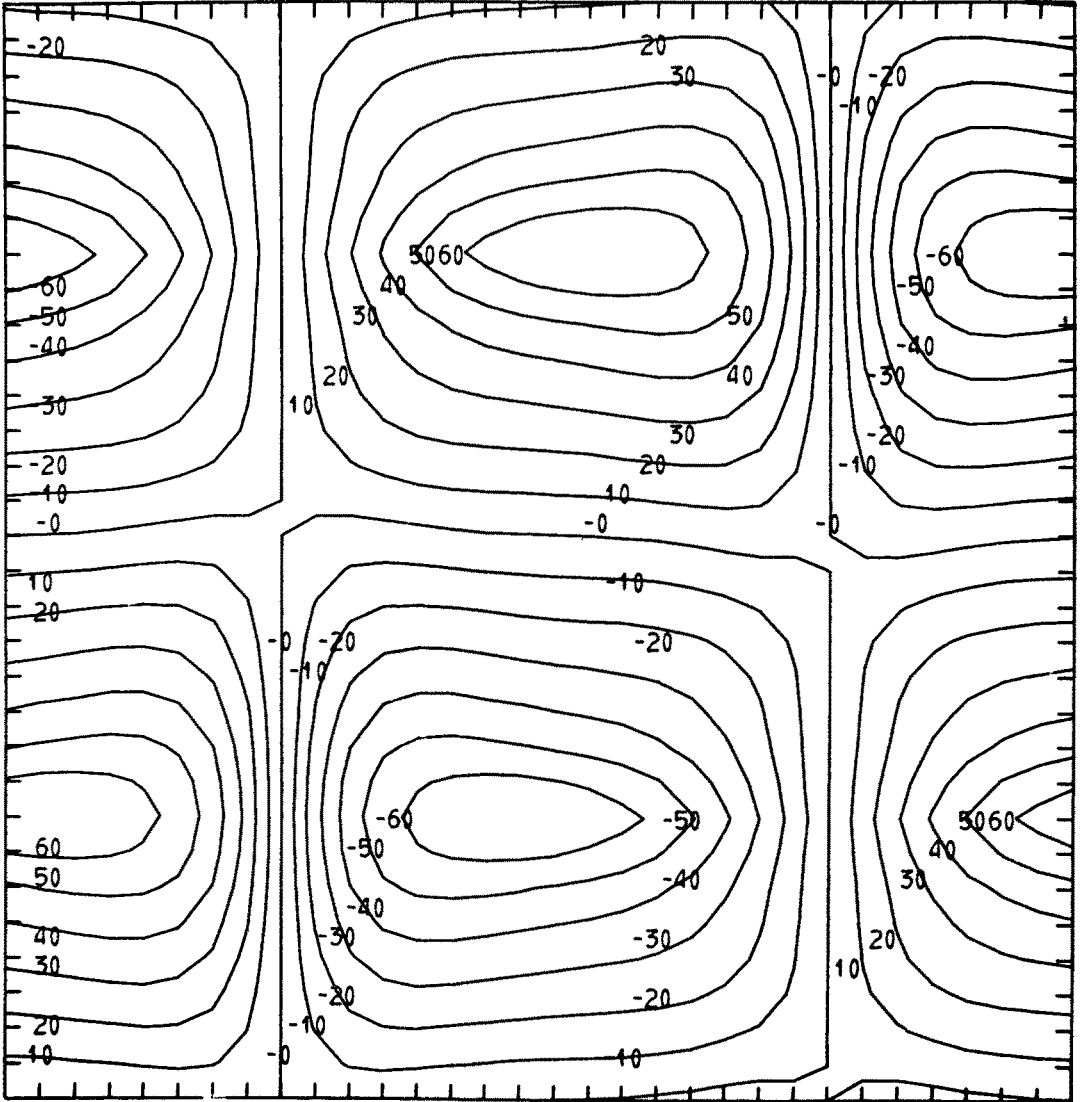
Fig. 4   Contour plot of v_1 at t = 3.5, R = 100 in the plane
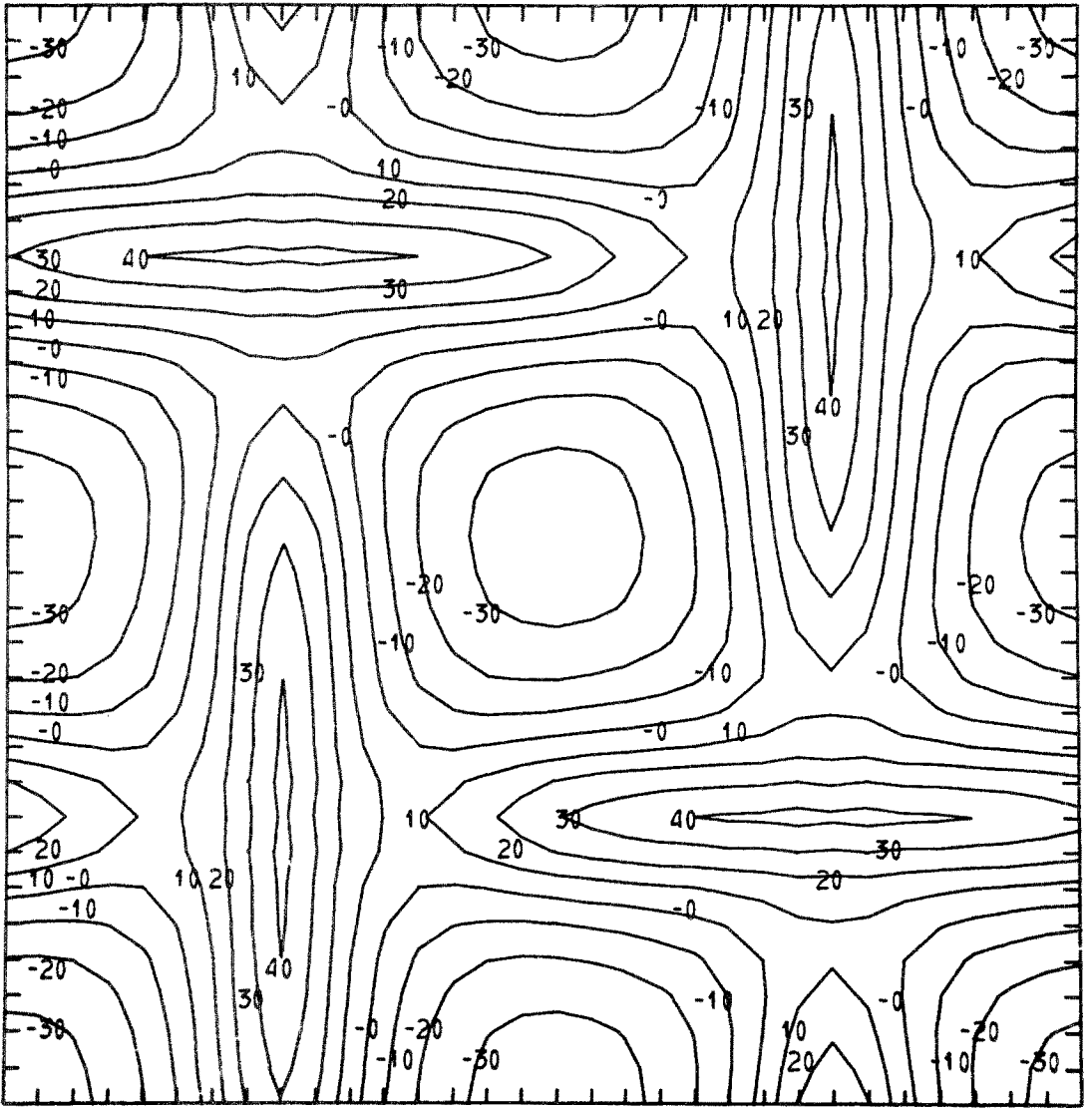$x_3 = \pi/4$.   The contour labels are $100v_1$.

V3

Fig. 5   Contour plot of v_3 at $t = 3.5$, $R = 100$ in the plane
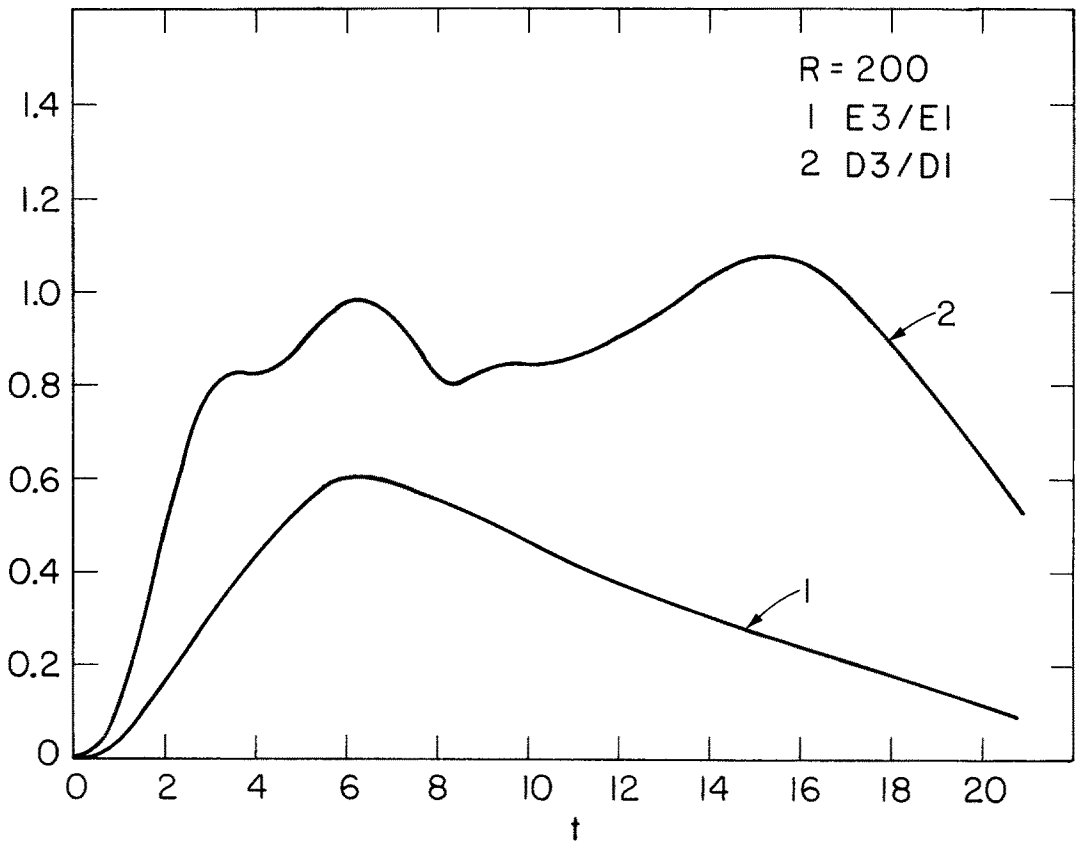$x_3 = \pi/4$. The contour labels are $100v_3$.

Fig. 6. Anisotropy ratios of kinetic energy and dissipation
versus t at R = 200.

smallest wavenumber, and hence smallest rate of viscous dissipation, dominate the flow. The smallest wavevectors allowed to have nonzero amplitude by the selection rules (8) are $\vec{k} = (\pm 1, \pm 1, \pm 1)$. The symmetry condition (8c) applied to the terms due to these $\vec{k}$ in the expansions (9) implies that $\vec{v}$ is proportional to its initial value (1) as $t \to \infty$. The net effect of nonlinearity in the Navier-Stokes equations is to speed the decay of (1); in the absence of nonlinearity; $\vec{v}$ would be forever proportional to (1) with amplitude $e^{-3t/R}$ [giving the R^0 term in the Reynolds expansion (6)].

REFERENCES

Batchelor, G. K., The Theory of Homogeneous Turbulence (Cambridge University Press, 1953).

Goldstein, S., Phil. Mag. 30, 85-102 (1940).

Orszag, S. A., Stud. in Appl. Math. 50, 293-327 (1971).

Orszag, S. A. and Israeli, M., Ann. Rev. Fluid Mechanics 6, xxx (1974).

Orszag, S. A. and Patterson, G. S., Phys. Rev. Letters 28, 76-79 (1972).

Taylor, G. I. and Green, A. E. Proc. Roy. Soc. A 158, 499-521 (1937).